Transactions, SMiRT-23
Manchester, United Kingdom - August 10-14, 2015
Paper ID 128

A Local Criterion to Predict Cleavage Crack Propagation and Arrest in a RPV Steel

Xiaoyu YANG[1,2], Clémentine JACQUEMOUD[1], Philippe BOMPARD[2], and Stéphane MARIE[3]

[1] CEA, DEN, DM2S, SEMT, LISN, 91191 Gif-sur-Yvette, FR
[2] Ecole Centrale Paris, Laboratoire MSSMat, Grande Voie des Vignes 92290 Chatenay-Malabry, FR
[3] AREVA, 1 Place Jean Millier, 92400 Courbevoie, FR

ABSTRACT

In this paper, a local criterion is proposed to predict cleavage crack propagation and arrest in a Reactor Pressure Vessel (RPV) steel. The objective is to develop an accurate predictive model, applicable and validated in the conditions of a thermal shock on a RPV steel.

A local stress based criterion has been proposed, derived from Ritchie Knott and Rice model. In this formulation, crack propagation and arrest are driven by a critical level of stress, at a given distance ahead of the crack tip. This critical stress has appeared to depend on temperature and plastic strain rate ahead of the crack tip.

In the first step, by using 2D modelling in Cast3M software, with extended finite element method, this criterion has been identified on isothermal fracture tests, performed on Compact Tensile specimens at different temperatures in the brittle-to-ductile transition range.

Then, in a validation step, the criterion has been successfully applied to predict the cleavage crack propagation and arrest on different specimen geometries, allowing mode I as well as mixed mode loadings and in both isothermal (at different temperatures) and anisothermal (i.e. thermal shock) tests. The results have therefore, demonstrated the transferability of the criterion for this steel, within a large range of thermal and mechanical loadings.

INTRODUCTION

The method defined by ASTM E1221 (2010) to predict crack arrest is based on a temperature dependent crack arrest toughness $K_{Ia}(T)$. Crack is supposed to propagate when the stress intensity factor in the vicinity of crack tip (K_I) reaches K_{Ia}, otherwise, crack arrest occurs. The value of $K_{Ia}(T)$ defined in ASME was obtained from an elastic-static analysis. It is questionable since it doesn't take into account some dynamic effects like the viscosity of material. Furthermore, the transferability of $K_{Ia}(T)$ is not always insured from one specimen geometry to another.

Local criterion, based on maximum principal stress (σ_I), has been used to predict the cleavage crack initiation. RKR criterion (R. O. Ritchie 1979) is one of the most well-known local criterion. According to it, crack is initiated when σ_I , at a given distance (r_c) ahead of crack tip, reaches a critical value (σ_{IC}). Inspired by this concept, some authors have proposed to use the same type of criterion to predict crack propagation and arrest (Hajjaj et al, 2006) (Dahl et al, 2011) (Prabel et al, 2007, 2008) (Bousquet et al, 2012, 2013). In Equation 1, crack begins to propagate when σ_I , at a given distance (r_c) ahead of crack tip, reaches a critical value (σ_{IC}), otherwise, it stops. In order to define σ_{IC}, two approaches were proposed recently: Hajjaj et al (2006) and Dahl et al (2011) proposed the dependence of σ_{IC} on temperature (T), and Prabel et al (2008) and Bousquet et al (2012) proposed its dependence on equivalent plastic strain rate ($\dot{\varepsilon}^p$).

$$f(\sigma) = \sigma_I - \sigma_{IC} = 0 \;\; \dot{a} > 0$$
$$f(\sigma) = \sigma_I - \sigma_{IC} < 0 \;\; \dot{a} = 0 \qquad \text{Equation 1}$$

Following previous work of Prabel (2008) and Bousquet (2012), the strain rate dependent local criterion is used in this paper to predict the crack propagation and arrest. This study aims to consolidate the criterion identification and to assess its transferability using different experimental configurations: for both mode I as well as mixed mode loadings and for both isothermal (at different temperatures) and multi-temperature (i.e. thermal shock) tests. All numerical works of this paper are based on analysis of tests by numerical simulations with eXtented Finite Elements Method (X-FEM) in Cast3M software (Cast3M, 2012).

CHARACTERIZATION OF MATERIAL

The RPV steel studied in this paper is 16MND5. Its chemical composition (Table 1) is near to those of A508 steel. The blocks have been taken from a French Pressurized Water Reactor (PWR) vessel ring ferrule. All specimens in this study are sampled in the way that, they were sollicited in the circumferential direction of the vessel, and the crack propagated in the thickness direction.

Table 1: Chemical composition of 16MND5

elements	C	Mn	Si	Ni	Cr	Mo	Cu
%(weight)	0.16	1.35	0.19	0.74	0.18	0.51	0.07

Mechanical behaviour of 16MND5

The material mechanical behaviour at high strain rate can be descried by Cowper-Symonds law (Equation 2): dynamic stress (σ_{dyn}) is the product of static stress (σ_{stat}) and a power function of plastic strain rate ($\dot{\varepsilon}^p$). σ_{stat} was obtained by isothermal quasi-static tensile tests from -175°C to 25°C (Chapuliot et al. 2005). The dependence of σ_{dyn} with temperature (T) is reflected through σ_{stat}, so there is no explicit temperature dependence. D and p are two parameters of material viscosity which can be identified by tests. They were identified by Bousquet (2012b) at five different temperatures (Table 2).

$$\sigma_{dyn}(\varepsilon^p, \dot{\varepsilon}^p, T) = \sigma_{stat}(\varepsilon^p, T)\left[1 + \left(\frac{\dot{\varepsilon}^p}{D}\right)^{\frac{1}{p}}\right] \qquad \text{Equation 2}$$

Table 2: Set of parameters (D, p) at five temperatures (Bousquet, 2012)

T°C	D(s^{-1})	p
-150	500 000	4.2
-125	31 000	6
-100	34 000	6.5
-75	16 000	7.2
-50	45 000	5.6

Thermal characteristics of the 16MND5 steel

The flowing thermal parameters are used for this study (Reytier et al. 2006) :

- Specific heat value (Cp) (Table 3): its values were measured by differential scanning calorimetry (DSC).
- Thermal conductivity (λ) (Table 3): its values were determined on the basis of measurements of Cp.
- Coefficient of thermal expansion (α) (Figure 1): it is a function of temperature (T).

Table 3: Specific heat value (Cp) and Thermal conductivity (λ) of the 16MND5 steel (Reytier et al. 2006)

Temperature (°C)	Specific heat Cp (J/kg/°C)	Conductivity λ (W/m/°C)
-175°C	275	29
0°C	450	39
100°C	500	39

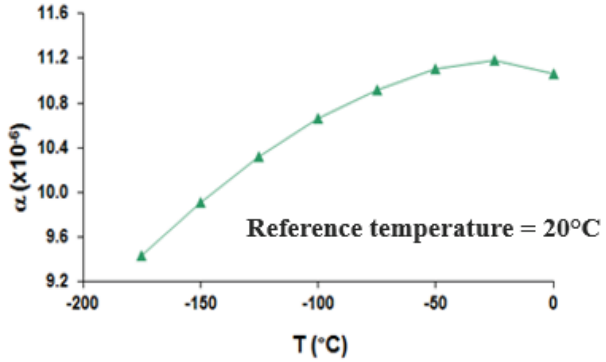

Figure 1. Evolution of the thermal expansion coefficient α as a function of the temperature (reference temperature = 20 ° C) for 16MND5 steel

CRITERION IDENTIFICATION

Isothermal tests on Compact Tension (CT25) specimens

Criterion identification has been performed on isothermal tests on CT25specimens. This type of specimen is recommended by ASME Standard E1820 to determine the toughness of the material. The measurement of crack propagation by camera requires a flat surface, so there is no side notch groove on these specimens. Their geometry is shown in Figure 2(b), crack can propagate for about 25 mm to reach its edge if its path is straight.

Tests have been performed on a 500 kN INSTRON tensile test machine. Figure 2(a) shows the test device. A thermal chamber is used to cool down specimen's temperature. Fifty three tests have been performed at four different temperatures: -150 ° C, -125 ° C, -100 ° C and -75 ° C. Major parts of this tests have been performed by Prabel (2008) and Bousquet (2012a). The reference temperature of Master Curves for this material is 121.8 ° C (Chapuliot et al. 2005). Under this condition, the main mechanism of crack propagation was cleavage. Crack propagation and arrest have been recorded by a high-speed framing camera (zone framed by red box) which makes the measurement of crack propagation more accurate. Figure 2(c) shows an example of crack growth recorded by this camera at a speed of 520 000 pictures/s. Generally, about 30 pictures are recorded for each test. Crack propagates about 25 mm during about 50 µs. The average speed is about 600 m/s and the maximum speed can attain around of 1000 m/s.

In addition to test temperature and all information about crack propagation (crack path, crack speed …), load and Crack Mouth Openning Displacement (CMOD) are also recorded for each test. Detailed information about this test can be found in (Yang et al. 2014).

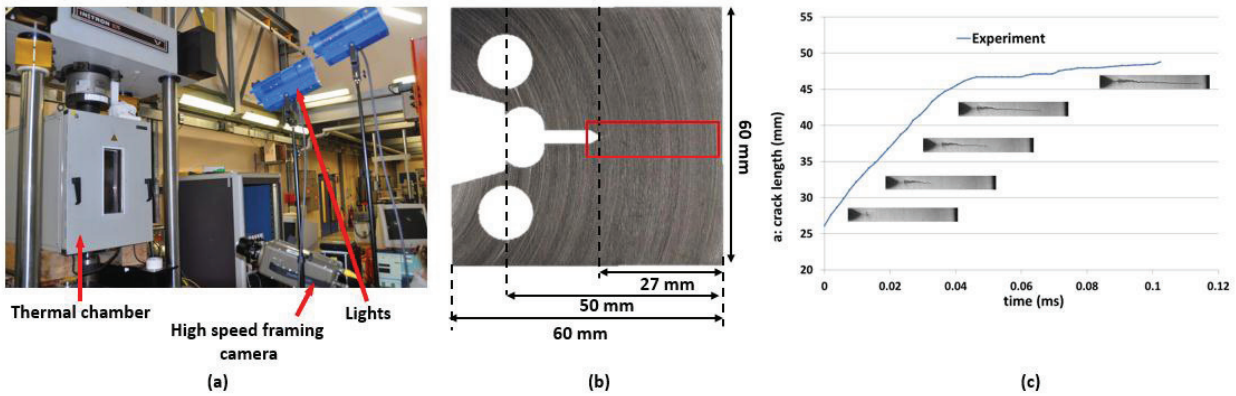

Figure 2. (a) Test device. (b) CT specimen geometry. (c) Crack growth recorded by high speed framing camera on 520HO3C (-150°C)

Numerical computation

Simulations are performed in 2D by eXtended Finite Element Method (X-FEM) with Cast3M software under hypothesis of plane strain and little deformation. Compared to classical Finite Element Method (FEM), X-FEM is more attractive, especially when the crack path is complex. In fact, the crack was meshed independently from that of specimen during the propagation. It means that we don't need to re-mesh the specimen at each step of crack propagation. Specific development were performed by Prabel (2007) to couple X-FEM models and elastic-plastic behaviour. Only one half of the CT25 specimen has been meshed because of symmetry (Figure 3). The mesh size was $(50 \times 50)\mu m^2$ along the crack path. This size is close to the microstructure entity of the material. The rest of specimen is meshed by standard elements. One elastic rod is modelled to simulate the stiffness of the testing machine.

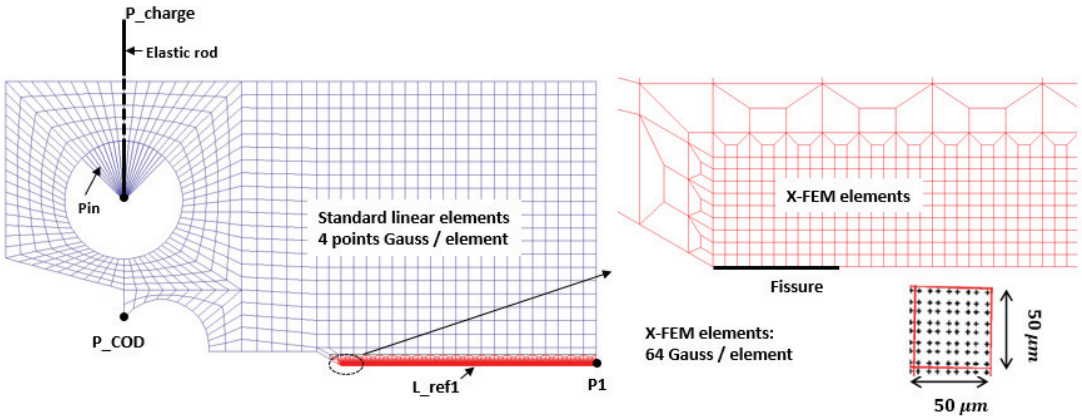

Figure 3. CT25 mesh

Simulation for each test is performed in two steps:

- Static loading: material behavior is elastic-plastic, this step is finished when CMOD calculated attains its experimental value.
- Dynamic crack propagation: material behavior is visco-plastic.

In the second step of simulation, dynamic crack propagation is reproduced numerically by imposing the crack growth evolution a(t) recorded by the high-speed framing camera during the test. At each calculation step, maximum principal stress (σ_I) and equivalent plastic strain rate $\dot{\varepsilon}^p$ at 100 µm ahead of crack tip are calculated and plotted in Figure 4 for the fifty three tests simulated at four different temperatures (from -150°C to -75°C).

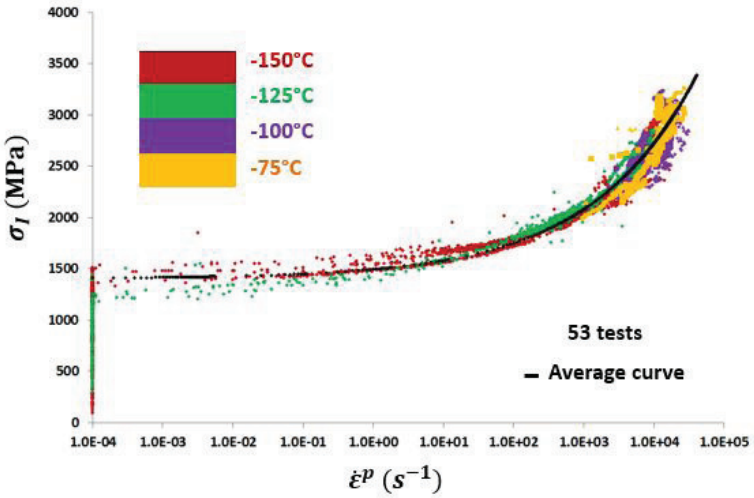

Figure 4. Identification of the RKR criterion

We can note from Figure 4 that:

- At low strain rate, maximum principal stress was nearly constant, and comparable to the cleavage fracture stress level generally identified for crack initiation. It increases dramatically at high strain rate.
- Influence of temperature is not obvious at high strain rate, however, its influence at low strain rate could exist and still needs to be confirmed.

The maximum principal stress plotted on Figure 4, corresponds to stress level necessary for the crack to propagate. For this reason, it could be associated to the critical stress σ_{IC}, because the crack propagates as soon as the maximum principal stress reaches this value. We could draw a trend line which passed in the middle of the results. This curve, described by Equation 3, could be considered as the crack propagation and arrest criterion.

$$\sigma_{IC} = \sigma_{IC0}\,[\,1 + 0{,}065(\dot{\varepsilon}^p)^{0{,}32}] \text{ for } r_c = 100\ \mu m \qquad \text{Equation 3}$$

with $\boldsymbol{\sigma_{IC0} = 1400MPa}$.

The dynamic critical stress σ_{IC} includes two parts: static critical stress (σ_{IC0}), which according to RKR criterion, is the stress necessary to separate crystal cleavage plan, and the other part could be considered as the viscosity force of material, it increases exponentially with equivalent plastic strain rate ($\dot{\varepsilon}^p$) in the vicinity of crack tip.

In order to test the validity and transferability of this criterion, it is then used to predict the crack propagation and arrest on some other specimens: isothermal ring specimen submitted to mixed mode loading and ring specimen submitted to thermal shock.

VALIDITY AND TRANSFERABILITY OF CRITERION FOR RING SPECIMENS SUBMITTED TO MIXED MODE LOADING (I+ II)

Tests on ring specimen submitted to mixed mode loading

Specimen dimension is shown on Figure 5(a). The ring specimen used for this test has inner diameter of 60 mm, outer diameter of 110mm and thickness of 25 mm. The angle between notch plan and specimen symmetry plan is 25°. Under compressive load, the crack is submitted to a mixed loading: both traction stress (mode I) and shear stress (mode II). Test device is the same as that for CT25. During each test, following parameters are recorded: test temperature, load, CMOD and all information related to crack propagation and arrest obtained from a high-speed framing camera (crack path, crack speed ...). The Figure 5(b) shows crack growth on test 520VV. Red frame represents the zone filmed during crack growth. The propagation lasted about 900 µs with an average speed of about 300 m/s.

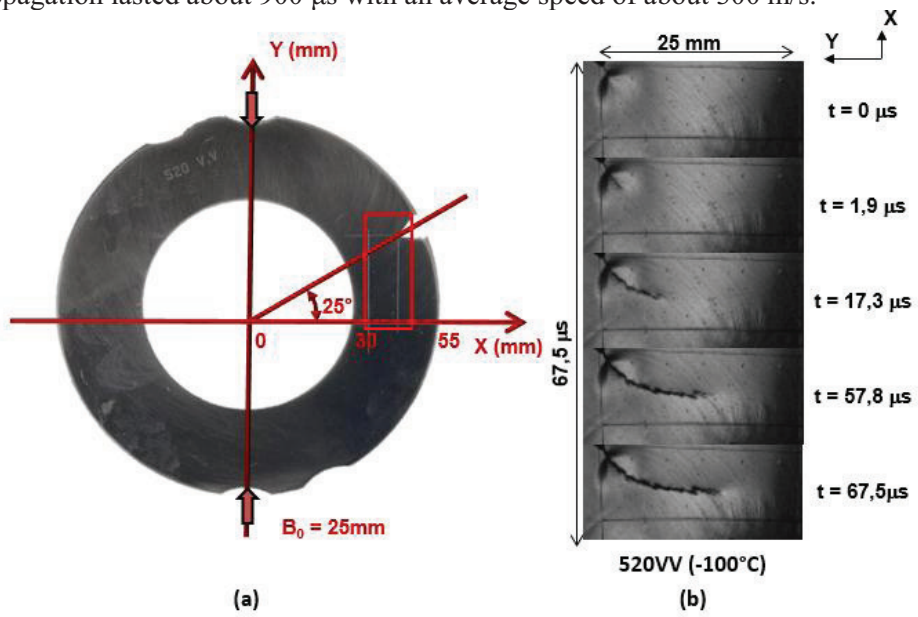

Figure 5. (a) Geometry of ring specimen under mixed mode loading. (b) Images of crack propagation recorded by high-speed framing camera at 440 000 i/s.

Three tests at different temperatures have been achieved: 520WE (-150°C), 520WA (-125°C) and 520VV (-100°C). Detailed information about these tests can be found in (Yang et al, 2014b).

Numerical computation

2D modeling was carried out with X-FEM, under hypothesis of plane strain and little deformation. Mesh for simulation is showed in Figure 6(a). Crack mesh is independent of the specimen's ones. The zone inside of which crack can propagate (in red color) is meshed with X-FEM elements, each element has a size of $(50 \times 50)\mu m^2$. The rest of specimen (in green color) is meshed with standard elements.

Simulation for each test is performed in two steps:

- Static loading: material behavior is elastic-plastic, the end of this step is defined by equivalence of energy according to Equation 4.

$$F(calc.) \times CMOD\ (calc.) = F(test) \times CMOD\ (test) \qquad \text{Equation 4}$$

- Dynamic crack propagation: material behavior is visco-plastic.

Here, we detail the second step of simulation. It is performed in a predictive way. Its principle is described in Figure 6(b): (x,y) is the local coordinate at crack tip, θ represents the angle. At each step of crack propagation, $\sigma_I(\theta)$ et $\dot{\varepsilon}^p(\theta)$ are calculated on a semicircle with a radius of 100µm. This allows us to get the maximum value of $\sigma_I(\alpha)$=(max[$\sigma_I(\theta)$]). Crack is supposed to propagate when max[$\sigma_I(\theta)$] reaches the critical stress (σ_{IC}) which depends on $\dot{\varepsilon}^p(\theta)$. σ_{IC} can be calculated according to the criterion identified (Equation 3). Otherwise, crack arrest occurs.

Since the crack path is not straight in ring specimen under mixed mode loading, an additional criterion is needed to predict crack propagation direction. In this paper, we suppose that the crack propagates in the direction normal to maximum hoop stress ($\sigma_{\theta\theta}$).

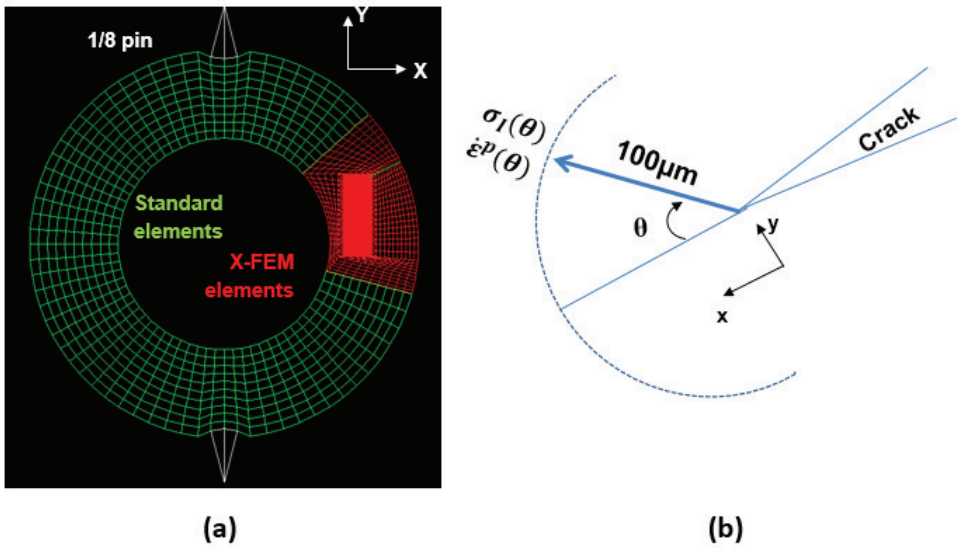

Figure 6. (a) Mesh of ring specimen under mixed mode loading. (b) Principle of predictive simulation on ring specimen under mixed mode loading.

The simulated results in terms of crack path and crack growth for three tests are showed in Figure 7. We find a good agreement between tests and simulations. It means that the criterion identified is applicable to predict the crack propagation and arrest on ring specimen under mixed mode loading. It shows also that the criterion is transferable from one specimen geometry (CT25) to another (ring specimen under mixed mode loading).

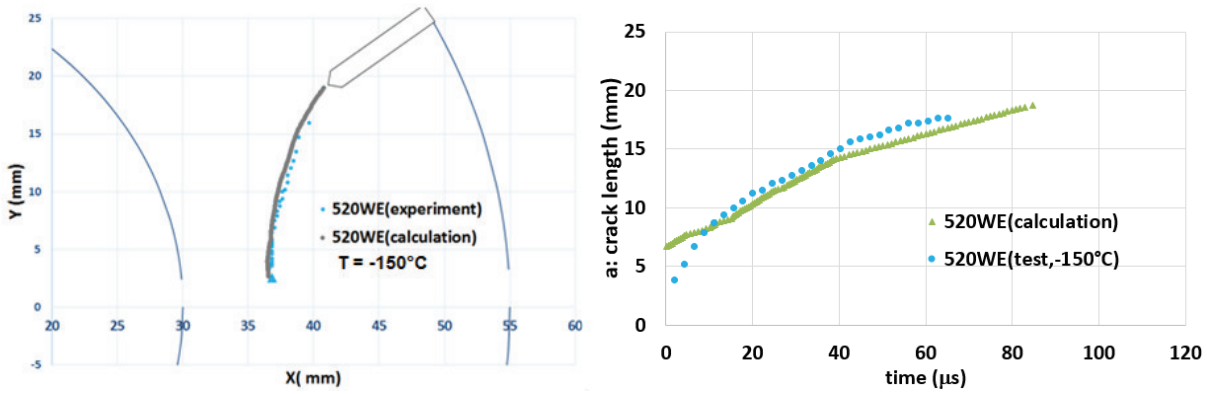

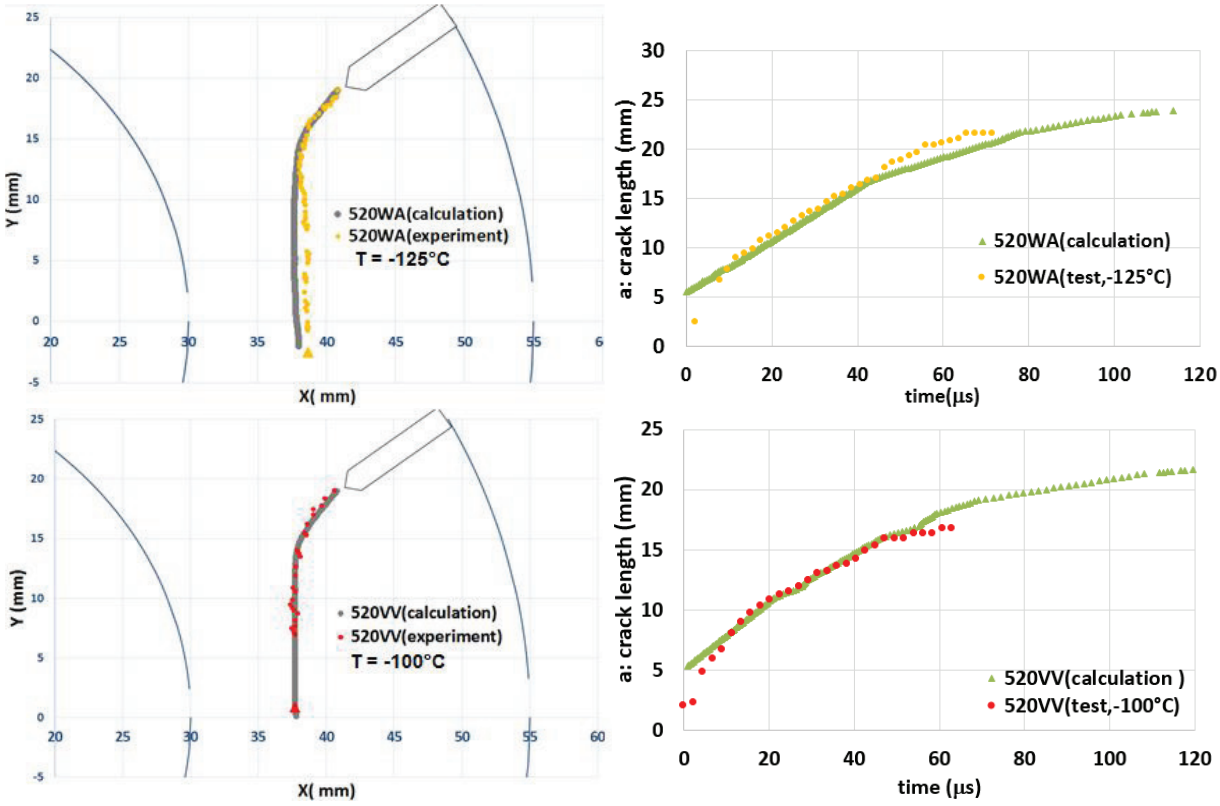

Figure 7. Comparison between simulations and test in terms of crack paths and crack growth for three ring specimens under mixed mode loading

VALIDITY AND TRANSFERABILITY OF CRITERION FOR RING SPECIMENS SUBMITTED TO THERMAL SHOCK

Tests on ring specimens submitted to thermal shock

Specimen dimension is shown on Figure 8(a). The ring specimen used in the thermal shock has inner diameter of 120 mm, outer diameter of 270 mm and thickness of 50 mm. Compared to CT25 and ring specimen submitted to mixed mode loading, this specimen is much bigger. There are 12 through holes in the specimen which allow the injection of water through the specimen thickness. The position of these holes was optimized to make the thermal load maximum.

The test presented in this paper (520LI-A) is subjected to complex loading: both mechanical loading and thermal loading. The test procedure can be described by the two curves showed on Figure 8(b): evolution of mechanical loading and CMOD recorded during the test. The ring is initially cooled down to -150 °C. Once the temperature is stabilized, a compressive loading is applied on the ring progressively up to 750kN, CMOD of ring specimen increase to 0.1mm during this mechanical loading. Then, the level of mechanical loading is maintained until the end of test, and hot water preheated to 90 ° C is injected through the holes. During this thermal loading, CMOD of specimen continues to increase by 0.1 mm and the crack initiates under thermal shock. Crack propagation and arrest are recorded by a high-speed framing camera at a speed of 440 000 pictures/s, which makes the measurement accurate. In fact, the thermal gradient in specimen thickness and the mechanical loading generate compressive stresses on inner surface of specimen, and the tensile stress at the crack tip. This configuration makes crack initiate and propagate under mode I. Thus, crack path is straight. Crack arrest occurs because it encounters a zone under compression and a material hotter therefore more tenacious.

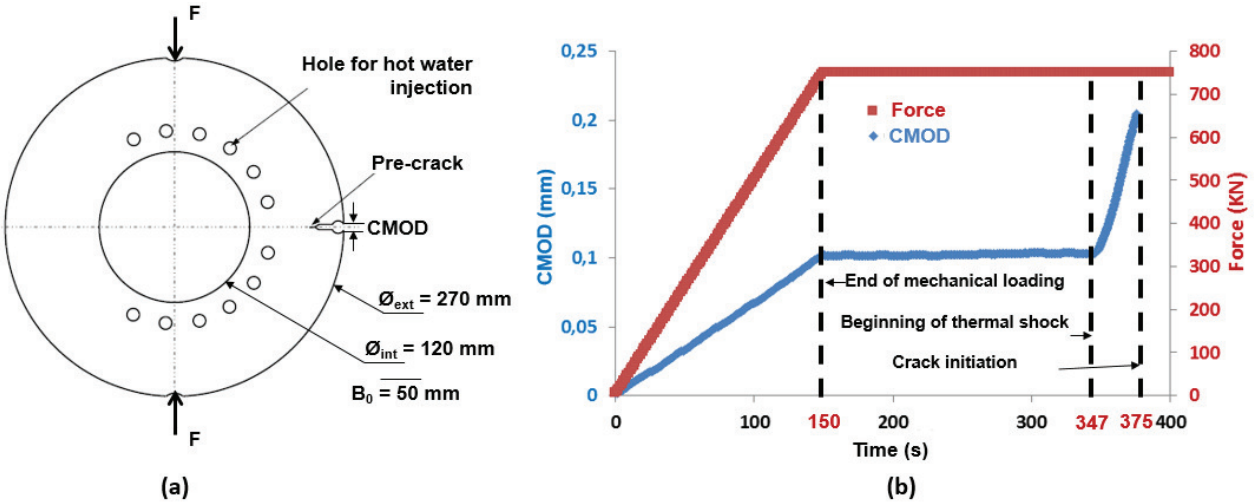

Figure 8. (a) Geometry of ring specimen for thermal shock test (b) Evolution of mechanical loading and CMOD during thermal shock test

Numerical computation

One half of the ring specimen submitted to thermal shock is meshed because of symmetry (Figure 9). The zone of crack path (in red color) is meshed with X-FEM elements with a size of $(50 \times 50)\mu m^2$, the same mesh size as for CT25 and ring specimen under mixed mode loading. The rest of specimen is meshed with standard elements.

2D modelling was carried out with X-FEM, under hypothesis of plane strain and little deformation. Simulation for each test is performed in three steps:

- Static mechanical loading: material behavior is elastic-plastic, the end of this step is defined by equivalence of mechanical loading between test and simulation.
- Static thermal loading: material behavior is elastic-plastic.
- Dynamic crack propagation: material behavior is visco-plastic.

Here, we detail the second and the third steps of simulation.

For static thermal loading, besides of parameters indicated in the second part of this paper: thermal conductivity (λ), specific heat values (Cp) and thermal expansion coefficient (α), we need also the coefficient of heat exchange by convection with air (h_{air}) and with hot water (h_{water}). Natural convection is imposed on the inner cylindrical surface, convection with hot water is imposed on the surface of holes. h_{air} is weak before h_{water}. For simplicity of calculation, we use $h_{air} = 400 \frac{W}{m^2}/°C$, value obtained by Reytier (Reytier et al. 2006). h_{water} is numerically optimized to accurately simulate the temperature variation of the twelve thermocouples within the ring. h_{water} optimized for test on 520LI-A is given in Table 4.

Table 4: Set of coefficient of heat exchange by convection with water

	h_{water} (T = -175°C)	h_{water} (T = +90°C)
520LI-A	1500	3000

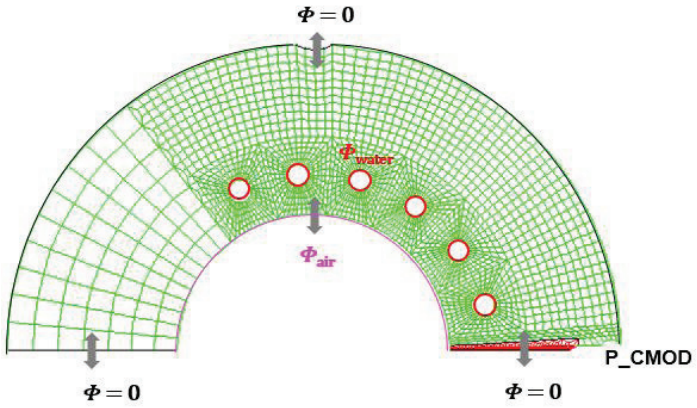

Figure 9. Mesh of ring specimen for thermal shock test and boundary conditions for thermal calculation.

The simulation of dynamic crack propagation is performed in a predictive way. At each step of simulation, we calculate the maximum principal stress (σ_I) and plastic strain rate ($\dot{\varepsilon}^p$) at 100µm ahead of crack tip. Crack propagates when σ_I reaches the critical stress (σ_{IC}) which depends on $\dot{\varepsilon}^p$, it can be calculated according to the criterion identified (Equation 3). Otherwise, crack arrest occurs.

Figure 10 shows crack growth predicted by criterion (curve in green color), it is in good agreement with test (curve in black color) in terms of crack length and propagation speed. It means that the criterion identified is applicable for ring specimen submitted to thermal shock and it is transferable from isothermal test to multi-temperature test. Evolution of temperature in vicinity of crack tip is described by the curve in red color. Temperature is between -150°C and -90°, it is included in the temperature range in which we have identified the propagation and arrest criterion.

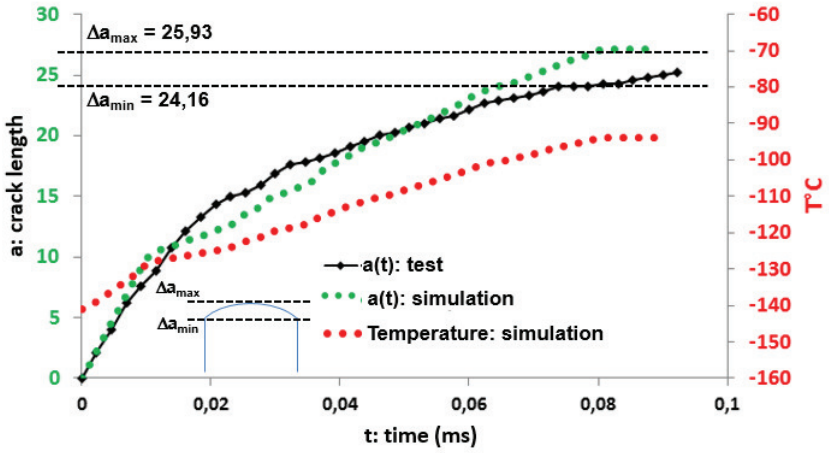

Figure 10. Comparison between test and predictive simulation for crack growth, evolution of temperature at the crack tip

CONCLUSION

A strain rate-dependent criterion, initially developed by Prabel (these) and Bousquet (Thèse), was presented in order to predict cleavage propagation and arrest in a reactor pressured vessel steel (16MND5). This criterion is derived from Ritchie Knott and Rice model: crack propagated as soon as the maximum principal stress σ_I , at a given distance ($r_c = 100\mu m$) ahead of crack tip, reaches a critical value (σ_{IC}) which depends on the equivalent plastic strain rate ($\dot{\varepsilon}^p$).

In the first step, by using 2D simulation in Cast3M software, with extended finite element method, this criterion has been identified on isothermal fracture tests, performed on fifty three Compact Tensile specimens at four temperatures: -150°C, -125°C, -100°C and -75°C. Simulated results showed that critical stress (σ_{IC}) increased with equivalent plastic strain rate ($\dot{\varepsilon}^p$), especially at high stain rate. Influence of temperature was not obvious at high strain rate. The criterion can be defined by a curve passing in the middle of simulated results.
Then, the identified criterion was applied to predict crack propagation and arrest on ring specimen under mixed loading. Three tests were carried out at different temperatures: -150°C, -125°C and -100°C. Simulation was performed in a predictive way. Results of simulation showed a good agreement with tests in terms of crack path, crack length and crack propagation speed.

Finally, the criterion identified was applied to predict crack propagation and arrest on ring specimen submitted to thermal shock (). This ring specimen is submitted to both mechanical loading (-750kN) and thermal loading. The thermal shock was generated by injecting hot water (90°C) through the thickness of ring specimen (-150°C). Crack growth and crack propagation speed predicted by the criterion were in good agreement with test.

Those results demonstrate the relevance and the transferability of the criterion to predict crack propagation and arrest under mixed mode loading condition or under thermal shock.

ACKNOWLEGEMENTS

The authors would like to thank T. Yurizinn and the LISN team for their contribution in this work. A special thank also to T. Le Grasse.

REFERENCES

ASTME1221, 2010American Society for Testing and Material - Standard Test Method for Determining Plane-Strain Crack Arrest Fracture Toughness, KIa, of Ferritic Steels, ASTM E1221, 2010.

Bousquet, S. Marie, and Ph. Bompard. 2012a. Cleavage Crack Propagation and Arrest in a Nuclear Pressure Vessel Steel. ASME PVP, Toronto, Canada.

Bousquet, S. Marie, and Ph. Bompard. 2012b. “Propagation and Arrest of Cleavage Cracks in a Nuclear Pressure Vessel Steel.” Computational Materials Science 64 (November): 17–21.

Bousquet A., Critère de propagation et d’arrêt de fissure de clivage dans un acier de cuve REP, PhD Thesis, Ecole Centrale de Paris, 2013.

Cast3M, 2012, Finite Element software developed by the French Atomic Energy Commission, http://www-cast3m.cea.fr.

Chapuliot, S., M. H. Lacire, S. Marie, and M. Nédélec. 2005. “Thermomechanical Analysis of Thermal Shock Fracture in the Brittle/ductile Transition Zone. Part I: Description of Tests.” Engineering Fracture Mechanics 72 (5): 661–73.

Dahl, A., C. Berdin, and D. Moinereau. 2011. “Dynamic Modeling of Cleavage Crack Propagation and Arrest with a Local Approach.” Procedia Engineering 10: 1853–58.

Hajjaj, M., 2006, “Propagation et arret de fissure dans les cuves de reacteurs a eau pressurisee”, PhD thesis, Ecole Centrale de Paris, France.

Prabel, B., S. Marie, and A. Combescure. 2008. “Using the X-FEM Method to Model the Dynamic Propagation and Arrest of Cleavage Cracks in Ferritic Steel.” Engineering Fracture Mechanics 75 (10): 2984–3009.

Prabel, B., Modélisation avec la méthode X-FEM de la propagation dynamique et de l’arrêt de fissure de clivage dans un acier de cuve REP, PhD Thesis, Institut National des Sciences Appliquées de Lyon, 2007.

Reytier, M., S. Chapuliot, S. Marie, L. Ferry, and M. Nedelec. 2006. “Study of Cleavage Initiation under Thermal Shock by Tests on Cracked Rings and Thermomechanical Calculations.” Nuclear Engineering and Design 236 (10): 1039–50.

R. O. Ritchie, W. L. Server. 1979. “Critical Fracture Stress and Fracture Strain Models for the Prediction of Lower and Upper Shelf Toughness in Nuclear Pressure Vessel Steels” 10 (10): 1557–70.

Yang, Xiaoyu, Stéphane Marie, Philippe Bompard, and Clémentine Jacquemoud. 2014. “Cleavage Crack Propagation and Arrest Prediction in French PWR Vessel Steel,” July, PVP2014-28422.

Yang, Xiaoyu, Stéphane Marie, and Clémentine Jacquemoud. 2014. “Cleavage Crack Path Prediction in a PWR Vessel Steel,” July, PVP2014-28418.